

tional discharge at 1.5 Tesla and 745 amp and a diffuse discharge at 1.53 Tesla and 1580 amp. Results for similar conditions obtained with high-speed framing cameras have also indicated the existence of a diffuse discharge at around atmospheric pressure.²

The existence of diffuse discharges at atmospheric pressure has been specifically investigated³ as part of a research programme on the development of high power plasma torches for industrial processes.⁴ The experimental set up comprised two parallel copper co-axial electrodes with an outer electrode bore of 20.8 mm and a radial separation of 8 mm in an axial magnetic field of up to 1.75 Tesla. A pulsed d.c. supply of up to 2100 amp was used of sufficient duration for the arc to reach equilibrium conditions. Initial observations using a high-speed framing camera indicated that the annular gap was apparently filled with a diffuse discharge. Results obtained with an optical probe indicated that the discharge became diffuse at rotational frequencies of about 20,000 Hz.

It was decided that a conclusive test was to detect the magnetic field due to the discharge current using a coil probe. A uniform diffuse discharge would produce no output voltage, an unstable discharge fluctuating between a diffuse discharge and a constricted discharge would produce an irregular output. If the discharge remained constricted at all times a regularly fluctuating output consistent over the whole range including that over which optical methods indicated that the arc was constricted should be obtained. Accordingly a search coil with a ferrite core was constructed. The coil comprised 86 turns of 42 SWG wire on a ferrite core 1.8 mm diam and 2 mm long. The coil was mounted with its axis midway between the electrodes and insulated from the discharge by a thin sheet of mica and a boron nitride cap. The optical probe was also mounted on the same support. An oscilloscope with four separate input channels was used to measure simultaneously the output from the two probes, the arc voltage and the arc current.

The output from the search coil indicated that the discharge remained constricted over the entire operating range. The measurements of velocity and rotational frequency over the lower range of rotational frequency were consistent with those obtained with the optical probe. No evidence of a transition was obtained.

The variation of arc velocity and rotational frequency with the magnetic flux density at various values of arc current are shown in Fig. 1, together with the measured value of velocity obtained by Garrison and Smith. (The rotational frequency is different due to the variation in electrode geometry.) The variation of arc voltage with magnetic flux density was measured and the increase in arc voltage with arc current at high currents noted by Garrison and Smith was also observed. The results for the measured arc velocity using a magnetic probe and the arc voltage have been compared with values of arc velocity of discharges which were known to be constricted and were found to be consistent with them⁵; no discontinuity either in arc velocity or arc voltage, which might be expected to occur at the transition from a constricted arc to a diffuse arc occurred.

More recent results⁶ using a camera with a framing rate of about 47,000 frames/sec and duration of exposure of 4 μ sec with a similar co-axial electrode arrangement indicate that with a photographic system capable of high optical definition a constricted arc in air can be defined under similar conditions to those reported by the author and Garrison and Smith.

Various possible mechanisms for the persistence of luminousness of an arc exist. Acoustic measurements of the decrease in arc temperature after arc interruption for arc currents up to 25 amp in air at atmospheric pressure indicate that the temperature decreases from about 6000°K to 4000°K within 100 μ sec after interruption of the arc current.⁶ The effect of increase in arc current and electrode separation may be expected to result in an increase in duration of the luminous-

ity. The luminosity of an arc due to ionisation below about 4000°K is negligible.

An alternative possible mechanism for the persistence of the luminosity of the discharge is the formation of active nitrogen.⁸ Although the lifetime of active nitrogen can be in excess of 1/2 hr at low pressures at atmospheric pressure its lifetime will be greatly reduced, nevertheless the lifetime is still sufficient to observe it as a jet when active nitrogen is discharged from a vessel into air.^{7,8} The lifetime will, however, be further reduced by the presence of other gases and may account for the ability to discern a constricted arc in air with improved optical techniques, apparently not possible in nitrogen alone.

References

- ¹ Garrison, G. W. and Smith, R. T., "Characteristics of a Magnetic Annular Arc Operating Continuously at Atmospheric Pressure," *AIAA Journal*, Vol. 8, No. 9, Sept. 1966, pp. 1714-1715.
- ² Mayo, R. F. and Davis, D. D., "Magnetically Diffused Radial Electric Arc Heater Employing Watercooled Copper Electrodes," Reprint 2453-62, 1962, ARS.
- ³ Harry, J. E. and Guile, A. E., "Constricted or Diffuse Arcs Rotating in High Magnetic Fields in Air at Atmospheric Pressure," *Proceedings of the Institution of Electrical Engineers (London)*, Vol. 115, No. 7, July 1968, pp. 1019-1023.
- ⁴ Harry, J. E., "A Power Frequency Plasma Torch for Industrial Heating," *Institute of Electrical and Electronic Engineers Transactions on Industrial and General Applications*, Vol. IGA-6(1), Jan/Feb. 1970, pp. 36-42.
- ⁵ Koetzold, B. R., "Rotierende Lichtbögen in gekreuzten elektrischen und magnetischen Feldern," *Elektrotechnische Zeitschrift*, Vol. 90, No. 22, 1969, pp. 587-589.
- ⁶ Edels, H. and Holme, J. C., "Measurement of the Decay of Arc Column Temperature Following Interruption," *British Journal Applied Physics*, Vol. 17, 1966, pp. 1595-1606.
- ⁷ Strutt, R. J., "An Active Modification of Nitrogen—VII," *Proceedings of the Society (London)*, Ser. A, Vol. 92, 1916, pp. 438-450.
- ⁸ Lehmann, K., Schulz, H., and Winde, B., "Nachleuchten von Stickstoffmolekülen bei Atmosphärendruck," *Zeitschrift für Physikalische Chemie (Leipzig)*, Vol. 205, 1956, p. 178.

Laminar Convective Heat-Transfer Rates on a Hemisphere Cylinder in Rarefied Hypersonic Flow

DAVID E. BOYLAN*

ARO, Inc., Arnold Air Force Station, Tenn.

Nomenclature

- C_p = specific heat at constant pressure
 C = linear viscosity relationship, $(T_\infty/\mu)(\mu^*/T^*)$
 e = Davis' parameter $[\bar{\mu}/(\rho_\infty U_\infty r_n)]^{1/2}$
 H_o = stagnation enthalpy
 H_w = wall enthalpy
 K^2 = Cheng's parameter, $p_\infty r_n/\mu_\infty U_\infty C$
 M_∞ = freestream Mach number
 p_o = total pressure
 p_∞ = freestream pressure
 Q_o = stagnation point heat-transfer rate
 Q_{1-4} = heat-transfer rate at various surface positions (Fig. 3)

Received February 5, 1971; revision received April 23, 1971. This work was sponsored by the Arnold Engineering Development Center (AEDC), Air Force Systems Command (AFSC), under Contract F40600-71-C-0002 with ARO, Inc., Arnold Air Force Station, Tenn.

*Engineer, Hypervelocity Branch, von Kármán Gas Dynamics Facility (VKF).

- r_n = nose radius
- Re_∞ = freestream unit Reynolds number, $\rho_\infty U_\infty / \mu_\infty$
- Re_2 = shock unit Reynolds number, $\rho_\infty U_\infty / \mu_2$
- s = surface distance measured from stagnation point
- St_o = stagnation point Stanton number, $Q_o / \rho_\infty U_\infty (H_o - H_w)$
- T_o = stagnation temperature
- T_w = wall temperature
- T_2 = temperature behind a normal shock
- T^* = reference temperature, $(T_2 + T_w) / 2$
- U_∞ = freestream velocity
- γ = ratio of specific heats
- μ_∞ = freestream viscosity
- $\bar{\mu}$ = viscosity as a function of U_∞^2 / C_p
- μ_2 = viscosity as a function of conditions downstream of a normal shock
- μ^* = viscosity as a function of T^*
- ρ_∞ = freestream density

I. Introduction

EXPERIMENTAL results are presented for the stagnation point heat-transfer rate and the heat-transfer rate distribution over a hemisphere-cylinder in hypersonic, rarefied flow. Comparison is made with the higher order theories of Cheng¹ and Davis² for the stagnation point heat-transfer rate and the theory of Lees³ for the heat-transfer rate distribution.

II. Apparatus and Results

A 2-in.-diam hemisphere cylinder instrumented with steady-state Gardon⁴ heat transfer gages was tested in a hypersonic low-density wind tunnel at AEDC (VKF Tunnel M). Both a conical nozzle and a contoured nozzle were used in the investigation. Test section core diameter varies from 5-10 in. Flow conditions and tabulated test results are given in Table 1. The data from the conical nozzle have been corrected for a small source flow effect.

The modified boundary-layer theory of Fay and Riddell⁵ provides a very good prediction of real gas stagnation point heating rates at altitudes for which slip effects (shock and wall) may be neglected. The failure of this method at a lower Reynolds number has been documented⁶ and confirmed by the present results. At a very low Reynolds number the Fay-Riddell theory estimates stagnation heating rates considerably above experimental values, while at a moderate Reynolds number, a slightly lower value is calculated.⁶ The purpose of this note is to compare higher-order theories with new experimental data.

The thin shock layer theory of Cheng¹ takes into account heat conduction and viscous effects immediately behind the bow shock. Direct application to the flow regime of the present study should be possible. Cheng points out that the analysis should fail when the continuum thin shock model cannot be assumed. He proposed a region defined by the

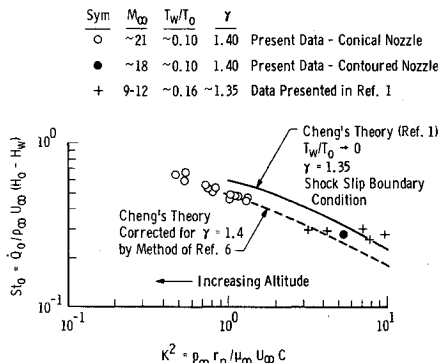


Fig. 1 Stagnation point heat-transfer rate data compared with Cheng's thin shock model.

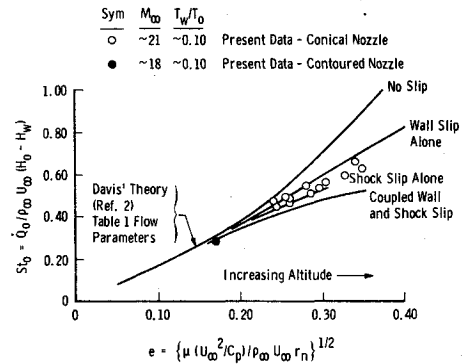


Fig. 2 Stagnation point heat-transfer rate data compared with the viscous shock layer theory of Davis.

parameter

$$K^2 = \rho_\infty r_n / \mu_\infty U_\infty C \gg 0(1)$$

as satisfying the basic assumptions employed in the analysis. This parameter is related directly to a local Reynolds number and inversely to the Knudsen number. The present experimental results are compared with Cheng's calculation in Fig. 1. The Mach 9-12 data shown by Cheng are in good agreement with his calculation for $K^2 \gtrsim 10$ but tends to fall below his solution in the range of the present data as shown in Fig. 1. Agreement between Cheng's theory and the present experimental results is good when differences in density ratios are taken into account. This correction follows the procedure of Potter⁶ and illustrates the sensitivity of density ratio on heat transfer in the stagnation region of blunt bodies. Data obtained in a hypersonic shock tunnel⁷ with equilibrium air ambient conditions indicate this same strong dependency. The present data are within the data band of this earlier work.

A numerical method similar to Cheng's developed by Davis² includes the separate and coupled influences of wall and shock slip. Agreement between the results of Cheng and Davis is quite good for calculations performed for the same flow and boundary conditions. Numerical results were obtained using a modified version of Davis' computer program[†] with the conditions of no slip, wall slip, shock slip, and combined wall and shock slip boundary conditions. Input data were the average values from Table 1. The results are shown in Fig. 2. The present data and theory are presented as a function of the parameter

$$e = [\bar{\mu} / \rho_\infty U_\infty r_n]^{1/2}$$

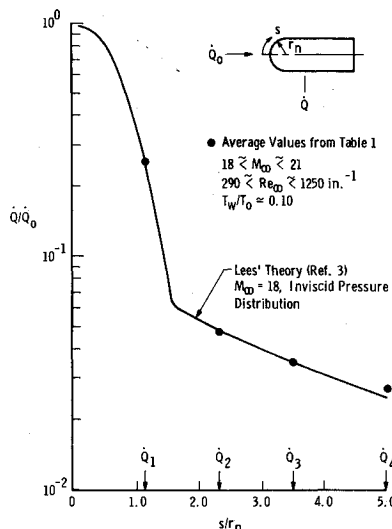


Fig. 3 Surface heat-transfer rate distribution on a hemisphere cylinder.

† Calculations were performed by E. O. Marchand, Special Studies Group, Hypervelocity Branch, VKF, AEDC.

Table 1 Flow conditions and test results

| p_0 , atm | T_0 , °K | H_0 , Btu/lbm | T_w/T_0 | M_∞ | Re_∞ , in. ⁻¹ | Re_z , in. ⁻¹ | \dot{Q}_0 , Btu/ ft ² /sec | S_{10} | See Fig. 3 | | | |
|-----------------|---------------|--------------------|-----------|------------|------------------------------------|-------------------------------|--|----------|-----------------------|-----------------------|-----------------------|-----------------------|
| | | | | | | | | | \dot{Q}_1/\dot{Q}_0 | \dot{Q}_2/\dot{Q}_0 | \dot{Q}_3/\dot{Q}_0 | \dot{Q}_4/\dot{Q}_0 |
| 13 | 3100 | 1615 | 0.10 | 21.1 | 450 | 14.4 | 7.71 | 0.53 | 0.25 | 0.047 | 0.034 | ... |
| 15 | 2200 | 1110 | 0.14 | 21.4 | 810 | 22.6 | 5.28 | 0.44 | 0.25 | 0.052 | 0.038 | ... |
| 17 | 2830 | 1460 | 0.11 | 21.5 | 640 | 19 | 7.37 | 0.46 | 0.26 | 0.047 | 0.036 | ... |
| 13.5 | 2305 | 1165 | 0.14 | 21.4 | 690 | 19.5 | 5.39 | 0.48 | 0.26 | 0.052 | 0.038 | ... |
| 16 | 3250 | 1700 | 0.10 | 21.4 | 490 | 15.5 | 8.48 | 0.50 | 0.26 | 0.049 | 0.036 | ... |
| 15 | 4100 | 2190 | 0.08 | 21.3 | 350 | 11.5 | 11.26 | 0.59 | 0.26 | 0.045 | 0.034 | ... |
| 13 | 3100 | 1615 | 0.11 | 21.3 | 450 | 13.7 | 7.65 | 0.56 | 0.22 | 0.046 | 0.034 | 0.029 |
| 12 | 4150 | 2225 | 0.08 | 20.8 | 290 | 10.1 | 10.90 | 0.63 | 0.27 | 0.047 | 0.034 | 0.028 |
| 17 | 2830 | 1460 | 0.12 | 21.4 | 640 | 19.5 | 8.11 | 0.49 | 0.25 | 0.045 | 0.033 | 0.026 |
| 15 | 2200 | 1110 | 0.14 | 21.4 | 810 | 22.7 | 5.63 | 0.47 | 0.26 | 0.047 | 0.034 | 0.028 |
| 16 | 3250 | 1700 | 0.10 | 21.3 | 490 | 15.9 | 9.39 | 0.54 | 0.25 | 0.041 | 0.028 | 0.024 |
| 13.5 | 2305 | 1165 | 0.14 | 21.3 | 690 | 19.6 | 5.39 | 0.48 | 0.26 | 0.045 | 0.032 | 0.027 |
| 11 | 3510 | 1850 | 0.09 | 20.9 | 360 | 10.9 | 9.08 | 0.66 | 0.26 | 0.046 | 0.031 | 0.025 |
| 19 ^a | 2900 | 1500 | 0.11 | 18.15 | 1250 | 45 | 11.66 | 0.28 | 0.25 | 0.049 | 0.040 | 0.030 |

Test Gas—Nitrogen

^a Contoured nozzle. All other data from conical nozzle.

It can be shown that the Davis parameter e^2 is inversely proportional to Cheng's parameter K^2 and both are related to a local Reynolds number. Cheng's calculation should be compared with the solution of Davis' with the boundary condition of shock slip alone. The utilization of coupled wall and shock slip boundary condition results in an estimate substantially below experimental results.

The heat-transfer rate distribution along the surface of the model is shown in Fig. 3. Very good agreement with the theoretical calculation of Lees³ using an inviscid method of characteristics pressure distribution can be seen. This must be considered fortuitous to some extent. In the present case, both \dot{Q}_0 and \dot{Q} appear to be increased proportionally because of induced pressure effects. This may not necessarily be true at lower unit Reynolds numbers.

The present results indicate that higher order effects are significant on stagnation point heating rates in rarefied flow. Available theories are not completely adequate for quantitative estimates according to the present data. The conventional technique of Lees³ for calculating heat-transfer rate distribution appears to be adequate at these test conditions.

References

- Cheng, H. K., "Hypersonic Shock-Layer Theory of the Stagnation Region at Low Reynolds Number," CAL Rept. AF-1285-A-7, April 1961, Cornell Aeronautical Lab., Buffalo, N. Y.
- Davis, R. T., "Numerical Solution of the Hypersonic Viscous Shock-Layer Equations," *AIAA Journal*, Vol. 8, No. 5, May 1970, pp. 843-851.
- Lees, L., "Laminar Heat Transfer Over Blunt-Nosed Bodies at Hypersonic Flight Speeds," *Jet Propulsion*, Vol. 26, No. 4, April 1956, pp. 259-269.
- Gardon, R., "An Instrument for the Direct Measurement of Intense Thermal Radiation," *The Review of Scientific Instruments*, Vol. 24, No. 5, May 1953, pp. 366-370.
- Fay, J. A. and Riddell, F. R., "Theory of Stagnation Point Heat Transfer in Dissociated Air," *Journal of the Aeronautical Sciences*, Vol. 25, No. 2, Feb. 1958, pp. 73-85, 121.
- Potter, J. L., "The Transitional Rarefied-Flow Regime," *Rarefied Gas Dynamics*, Vol. II, Supplement 4, Academic Press, N. Y., 1967, pp. 881-937.
- Vidal, R. J. and Wittliff, C. E., "Hypersonic Low Density Studies of Blunt and Slender Bodies," *Rarefied Gas Dynamics*, Vol. II, Supplement 2, Academic Press, New York, 1963, pp. 343-378.